Journal of Applied and Natural Science
17(1), 389 - 397 (2025)
ISSN : 0974-9411 (Print), 2231-5209 (Online)
journals.ansfoundation.org

Research Article

Deep learning of backpropagation neural network algorithm for long-term predicting rainfall in the Kapuas Hulu, West Kalimantan province of Indonesia

Bobby Adhityo Rizaldi*
Department of Defense Science, Doctoral Program, Republic Indonesia Defense University, Indonesia
Anak Agung Banyu Perwita
Department of Defense Science, Doctoral Program, Republic Indonesia Defense University, Indonesia
Joni Widjayanto
Department of Defense Science, Doctoral Program, Republic Indonesia Defense University, Indonesia
M.Adnan Madjid
Department of Defense Science, Doctoral Program, Republic Indonesia Defense University, Indonesia

*Corresponding author. E-mail: bobbyadhityor@gmail.com

Article Info
https://doi.org/10.31018/jans.v17i1.6183
Received: September 14, 2024
Revised: March 07, 2025
Accepted: March 12, 2025

How to Cite
Rizaldi, B. A. *et al.* (2025). Deep learning of backpropagation neural network algorithm for long-term predicting rainfall in the Kapuas Hulu, West Kalimantan province of Indonesia. *Journal of Applied and Natural Science*, 17(1), 389 - 397. https://doi.org/10.31018/jans.v17i1.6183

Abstract
Climate change and global warming significantly impact rainfall patterns in various regions. This can lead to more frequent and intense flooding and an increased risk of landslides. As a result, it causes unstable rain variability patterns in various regions, including Kapuas Hulu, West Kalimantan Province, Indonesia. Almost every year, the area experiences floods and landslides. The area, directly adjacent to the Indonesia-Malaysia region, can potentially disrupt community activities, including military operations guarding the border, which require a lot of manpower. This study aimed to minimize future disasters as it is vital to anticipate rainfall patterns based on previous data from databases. The Backpropagation Neural Network (BPNN) approach is one of the best at predicting long-term rainfall. Rainfall data from NASA was utilized from January 2003 through December 2020, totalling 216 data sets. The input or training data ranges from January 2003 to December 2010, whereas the training goal data is from January 2011 to December 2015. The validation data was also determined from January 2016 to December 2020. With a learning rate of 0.3 and an Epoch of 9,999, the best predictive architecture model was 8-6-9-6-5. The prediction accuracy was pretty excellent, with a mean square error (MSE) of 0.012157 and a mean absolute percentage error (MAPE) of 24.026. The highest rainfall was recorded in December 2019 at 606.672 mm/month. The prediction results are expected to serve as a reference for mitigating disasters such as floods and landslides to facilitate security operations in border areas.

Keywords: Backpropagation Neural Network (BPNN), Disaster, Flood, Prediction, Rainfall

INTRODUCTION

Climate change and increasingly severe global warming have caused climate uncertainty globally, including in various regions of Indonesia. This results in fluctuations in rainfall patterns, making it difficult to predict rainfall (Oppenheimer *et al.*., 2016). This uncertainty in rainfall patterns has far-reaching implications for various sectors in Indonesia. However, using data mining techniques and utilizing past rainfall data as input, we can predict future rainfall more accurately. Data mining can process large amounts of data quickly and accurately, allowing it to predict future weather changes in Indonesia (Chauhan and Thakur, 2014). Rainfall is a very important environmental phenomenon in Indonesia, especially in the agricultural sector for crop production. The amount of rainfall significantly influences determining crop yields (Salman, 2016).

Previous research by Pratama *et al.*. (2021) predicted rainfall, tides, and topography based on the monthly

period. However, this period has certain weaknesses. For instance, several Indonesian Agency for Meteorological, Climatological and Geophysics monitoring stations in certain areas may lack records or have missing data due to malfunctioning recording devices. Kim *et al.*. (2019) mention that using a time period makes calculating missing data at specific times impossible. Rainfall is the amount of rainwater that falls on the Earth's surface during a specific period in a particular area. Rainfall can be measured over daily, monthly, or yearly periods. Several elements determine the amount of rainfall in a given place, including air humidity, air pressure, temperature, and wind speed. (Putra *et al.*., 2022). Although the exact amount of future rainfall cannot be determined with certainty based on historical data, it can be predicted using past rainfall data. However, detailed rainfall forecasts for each region are lacking (Todini, 2007). Accurate knowledge of rainfall is crucial for various sectors, including water supply management, reservoir maintenance, and flood control in a specific area (Hanak and Lund, 2012).

The rainfall prediction is important because it affects river discharge and can help mitigate the impact of rainfall-related disasters such as landslides. Heavy rainfall in mountainous regions can trigger disasters that impact public infrastructure, waste disposal networks, and other human activities. Therefore, accurate rainfall prediction is crucial for proper planning and risk management (Shi *et al.*., 2015). Backpropagation is a popular supervised learning method with advantages in terms of its learning capabilities. Historical data is utilized to identify short-term, medium-term, or long-term trends when forecasting future events. Backpropagation is suitable for making future predictions due to its straightforward calculation process and ability to handle complex data (Shirzadi *et al.*., 2021).

Artificial Neural Networks (ANN) are processing systems designed to mimic the workings of the human brain, enabling them to recognize patterns based on studied historical data and make decisions based on previously unseen data (Kukreja *et al.*., 2016).

One method that can be used to measure the magnitude of prediction error is MAPE. Utilizing the Mean Absolute Percentage Error (MAPE) helps obtain predictive results by minimizing errors and reducing uncertainty in the predicted data. MAPE represents the absolute error rate in predictions compared to actual values (Al Mamun *et al.*., 2020). BPNN has been successfully applied in various sectors, including predicting data encryption- decryption patterns (Shihab, 2006), cybersecurity decryption functions (Bapiyev *et al.*., 2017), solving intrusion detection problems (Afolabi and Aburas, 2021), predicting wind speed for wind power plants (Qu *et al.*., 2019), light intensity for solar power plants (Zhong *et al.*., 2018), and rainfall (Guha *et al.*., 2022). Based on the problem description, a study on Rainfall Long-term Prediction in Kapuas Hulu, West Kalimantan, is proposed using the backpropagation neural network algorithm based on rainfall determinants. Therefore, this study focused on predicting rainfall in Kapuas Hulu in Indonesia, an area with extremely high rainfall intensity that is prone to flooding and landslides.

MATERIALS AND METHODS

The study utilized data related to weather conditions in the sub-district, such as temperature, humidity, altitude, area, number of mountains, green area, distance from the sea, water availability, and rainfall from 2003 to 2020. The data was divided into two categories: learning data and validation data. By collecting and analyzing this data, it is expected that the proposed system can provide early rainfall predictions to assist in addressing future disaster-related issues.

Data Source

The rainfall intensity data source used was from 2003-2020, with the distribution of training data from 2003-2010, followed by learning data from 2011-2015. The validation data was taken from 2016 to 2020, with data available for each month from January to December. The overall rainfall intensity data was obtained from "https://power.larc.nasa.gov/data-access-viewer/". The selected location was at point 0 in Kapuas Hulu, West Kalimantan, with the geographical coordinates Latitude 0.95 and Longitude 112.8833. The location was chosen in the city center to map rainfall patterns as a future mitigation effort.

Backpropagation Neural Network (BPNN)

Paul Werbos initially introduced the backpropagation neural network (BPNN) method. Werbos (1974) proposed the "backpropagation of error" algorithm in his dissertation titled "Beyond Regression: New Tools for Prediction and Analysis in the Behavioral Sciences". His contribution was recognized as a significant step in developing the backpropagation algorithm. Following that, David Rumelhart, Geoffrey Hinton, and Ronald Williams reconstructed the backpropagation method in a significant article titled "Learning representations by back-propagating errors" in 1986. This paper helped popularize the backpropagation algorithm and made it widely known and studied in the computer science and artificial intelligence communities.

The BPNN algorithm method fundamentally utilizes a multilayer network. This means that the architecture of the Backpropagation Neural Network typically consists of three types of layers: the input layer, the hidden layer, and the output layer. Each layer consists of several interconnected neurons. The input layer initially functions to transmit input signals X to the hidden layer, so

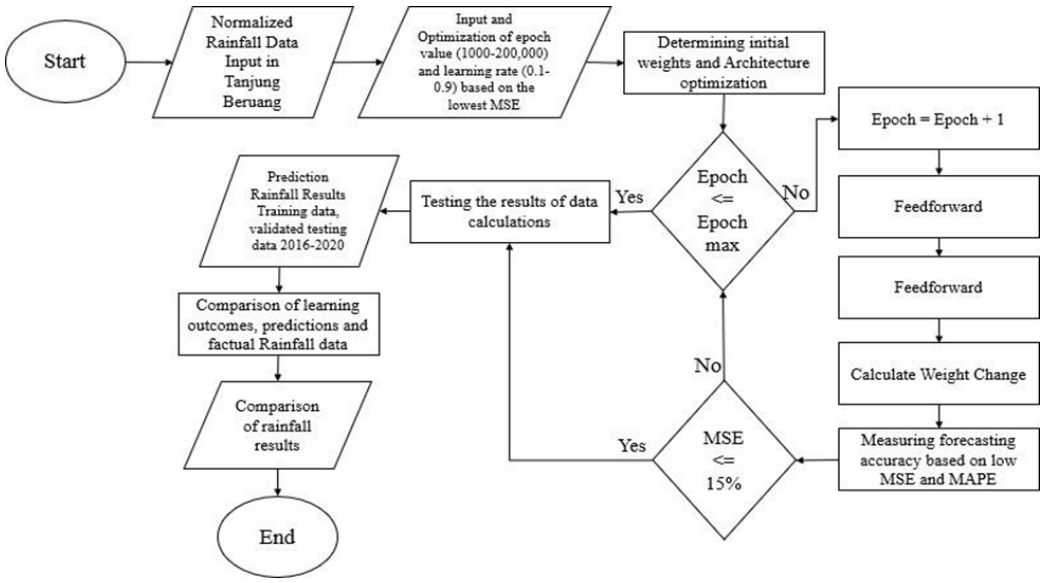

Fig. 1. *Long-term Backpropagation neural network flowchart*

no computation process has taken place yet. In the hidden layer, each neuron receives input from neurons in the previous layer and provides output to neurons in the next layer. The hidden layer plays a role in extracting and learning patterns in the input data. The output layer performs computations on the weights and biases and calculates the output values based on a specific activation function. Typically, a binary sigmoid activation function ranging from 0 to 1 is used (Karsoliya, 2012). The flowchart of the BPNN is mentioned in Fig. 1.

The following were the first steps in training the BPNN approach:

Began by assigning tiny random values to the weights.

If the MSE and MAPE halting requirements are not fulfilled, go to steps 3-8.

Step 1: Feed forward propagation

Each input unit (*xi*, *i*=1,.,n) receives input signals xi and forwards them to the hidden

units. Each input unit (x*i*, *i*=1, 2, 3, n) receives the signal Xi and passes it to

all units in the layers above it (hidden layers).

According to Fei J *et al.*. (2016), each hidden unit (zj, j=1,.....,p) sums the weighted input signals using equation (1).

$$Z = V_{0j} + \sum_{i=1}^{n} X_i V_{ij} \quad (1)$$

When Z is the hidden neuron, V0j is the bias weight from the input neuron to the j, and xi is the input neuron to the i. Vij is the weight of the input neuron to the hidden neuron.

Equation is used to apply and compute the activation function (2).

$$Z_j = f(Zin_j) \quad (2)$$

When Zj is a hidden layer unit to j, Zin_j is the output of Zj unit.

The sigmoid function, for example, is employed as the activation function in equation (3).

$$Y = f(x) = \frac{1}{1+e^{-x}} \quad (3)$$

This signal is sent to all units in the output layer via the sigmoid activation function.

Using equation, each output unit (yk, k = 1,. ,m) adds the weighted input signals (4).

$$Y_{ink} = w_{0k} + \sum_{k=1}^{p} z_j w_{jk} \quad (4)$$

With Y_ink being the output for the unit yk; w_0k being the bias weight for the hidden neuron to k; zj being the unit j in the hidden layer; and w_{jk} being the weight neuron hidden to output neuron.

Using the activation function derived by equation (5).

$Y_k = f(Yin_k)$ (5)

With. Y_{ink} is outpot for $Y_{k.}$ Unit.

Step 2: Backpropagation (backward)

The input training patterns are received by each output unit (yk, k=1,. ,m). Using the

equation, calculate the inaccuracy for each layer (6).

$\delta_k = (t_k - y_k)f'(y_{in}k)$ (6)

When δk is the weight correction factor wjk; t is target; yk is output neuron to k; $y_{in}k$ is output for yk unit.

Using equation, compute the weight and bias adjustments (7).

$\Delta w_{jk} = \alpha\delta_k x_j$ (7)

$\Delta w_{jk} = \alpha\delta_k$

When Δw_{jk} = is the difference between w_{jk} (t) with w_{jk} (t+1); Δw_{0k} is the bias weight for the hidden neuron to

the k; α is learning rate; δk is the weight correction factor.
wjk; x is input.
7. In each hidden unit (zj, j=1,….,p) It sums up the delta of its inputs (from units in the
higher layers) using equation (8).

$$\delta_{in_j} = \sum_{k=1}^{p} \delta_k w_{jk} \quad (8)$$

Where δ_k is the weight correction factor for wjk, and wjk is the weight neuron hidden to the output neuron. Using equation, calculate the inaccuracy for each layer (9).

$$\delta_j = \delta_{in_j} f(x_{in_j}) \quad (9)$$

When δ_j is the weight correction factor to v_{ij}; δ is correction factor; x is input.
Using the equation, compute the weight and bias adjustments (10).

$$\Delta v_{ij} = \alpha \delta_j x_i \quad (10)$$

With Δv_{ij} is the weight of the hidden neuron's input neuron.; α = learning rate; δ_j = the weight correlation coefficient v_{ij}; x_i = an input neuron to i.

Step 3: Update the weights and biases.
In each output units (yk, k=1,.....,m) Update the weights and biases (j = 0,1,..p) are calculated using equation (11).

$$w_{jk}(new) = w_{jk}(initial) + \Delta w_{jk} \quad (11)$$

Where w_{jk} is the weight from the hidden neuron to the output neuron.; Δw_{jk} is the weight difference between the hidden neuron and the output neuron.
In each hidden units (zj, j = 1,..,p) updating the weights and biases. (i = 0,1,..n) calculate with (12) equations.

$$v_{ij}(new) = v_{ij}(initial) + \Delta v_{ij} \quad (12)$$

Where vij is the weight transferred from the input neuron to the hidden neuron; Δv_{ij} is the weight difference between the input neuron and the hidden neuron.
Maximum input epochs to automatically stop.

Accuracy of Prediction
Validation to measure prediction accuracy uses the Mean Squared Error (MSE) method to evaluate forecasting errors for each period and divide it by the number of forecast periods used (Zhang *et al.*., 2015). The formula for calculating the MSE accuracy measurement can be seen in equation (13).

$$MSE = \frac{1}{n} \sum_{i=1}^{n} (r_i - \hat{r}\, i)^2 \quad (13)$$

Where Yi is actual value; $\hat{r}$ i is predict value; n amount of time periods or goals.
The value of Mean Absolute Percentage Error (MAPE) is used to select the optimal design optimization indicator (VanDeventer *et al.*., 2019). MAPE is a measure of prediction variability for statistical forecasting systems, commonly used to indicate the accuracy ratio determined by equation. (14).

$$MAPE = \frac{100\%}{n} \sum_{i=1}^{n} \left| \frac{A_t - F_t}{A_t} \right| \quad (14)$$

Data sample
The rainfall data from January 2003 to December 2020, totaling 216 sets of data, was obtained from NASA, making this research based on long-term data learning. It should be noted that the data from January 2003 to December 2010 is positioned as input data, and the Training Target Data is from January 2011 to December 2015. The validation data is determined from January 2016 to December 2020. Each data is normalized within the range of 0.1-0.9 using equation (15), and the normalized data results are shown in Table 1 and Fig. 2.

$$X' = \frac{0.8(X-b)}{(a-b)} + 0.1 \quad (15)$$

It is known that X' represents normalized data, a represents the highest value of factual data, b represents the minimum value of factual data, and X represents the factual data. Furthermore, the BPNN algorithm is used in the prediction phase. To retrieve the original form of the forecasts, the anticipated outcomes are denormalized. Equation shows the formula for computing denormalized data (16).

$$X = \frac{(X'-0.1)(b-a)+0.8a}{0.8} \quad (16)$$

RESULTS AND DISCUSSION

The prediction of rainfall data from 2016-2020 was conducted using the BPNN algorithm implemented in Python. The process involved optimization of the learning rate and epoch parameters to obtain the best results. These parameters produced the best values when the resulting MSE was significantly small, less than 10% (Chen G *et al.*., 2014). As a result, an optimization procedure was carried out by adjusting the learning rate from 0.1 to 0.9 and the number of epochs from 10,000 to 200,000 with a 10,000-step size. The graphical relationship between the optimization of epochs and the learning rate for the MSE values is shown in Fig. 3.
Fig. 3 illustrates that the ideal learning rate of 0.3 and epoch value of 9999 results in the lowest MSE value, with an MSE value of only 0.000716307355991353 (<

Table 1. Index rainfall of 2011-2015 period actual (Learning)

Month	Year				
	2011	**2012**	**2013**	**2014**	**2015**
Jan	0.540580985	0.343474915	0.355072623	0.320290492	0.876815577
Feb	0.349279266	0.586960823	0.708698281	0.175357619	0.372463688
Mar	0.540580985	0.737687054	0.436234592	0.436234592	0.569569758
Apr	0.384061396	0.453625658	0.575363115	0.302899427	0.633340662
May	0.395659104	0.302899427	0.563776401	0.494201146	0.360865981
June	0.494201146	0.256519588	0.204346392	0.291301719	0.41305017
July	0.320290492	0.453625658	0.384061396	0.146379839	0.221737458
August	0.198553035	0.505798854	0.418843527	0.604351889	0.262323939
Sept	0.308692784	0.291301719	0.505798854	0.436234592	0.227541808
Oct	0.598558531	0.563776401	0.29710607	0.430441235	0.389854754
Nov	0.500005497	0.87102222	0.44202795	0.865217869	0.760871477
Dec	0.9	0.639134019	0.778262542	0.482614431	0.4478323

Table 2. Index actual rainfall from 2016 to 2020 (Validate)

Month	Year				
	2016	2017	2018	2019	2020
Jan	0.55797205	0.500005497	0.488407789	0.540580985	0.528983277
Feb	0.621742954	0.598558531	0.482614431	0.586960823	0.471016723
Mar	0.540580985	0.401452462	0.650731727	0.32608385	0.575363115
Apr	0.563776401	0.4478323	0.604351889	0.511592211	0.598558531
May	0.615949597	0.476810081	0.679709508	0.279715004	0.436234592
June	0.563776401	0.430441235	0.511592211	0.430441235	0.482614431
July	0.32608385	0.378257046	0.279715004	0.244932873	0.656525085
August	0.256519588	0.720295989	0.273910654	0.343474915	0.41305017
Sept	0.569569758	0.685513858	0.239128523	0.192759677	0.523189919
Oct	0,476810081	0,482614431	0,749273769	0,453625658	0,41305017
Nov	0,471016723	0,621742954	0,592754181	0,29710607	0,546374342
Dec	0.436234592	0.528983277	0.563776401	0.760871477	0.360865981

0.10). This is consistent with the parameters reported by Wica *et al.*. (2019) with an MSE value of 0.0218 (also below 10%) using a learning rate of 0.7 and a 10.000 epoch. It should be emphasized, however, that the epoch and learning rate/alpha values are not universally relevant to all datasets but are only appropriate for certain datasets or locations with unique data patterns. As a result, before making predictions, Tarigan *et al.*. (2017) recommend optimizing the learning rate, hidden layer design, and epoch, as well as the learning rate, momentum rate, and number of hidden neurons simultaneously. This study also makes use of a parameter optimization system, which includes the learning rate, architecture, and a range of epochs in the hundreds of thousands and is backed up by an 18-year (long-term) database. Once all the optimization parameters we re obtained, the prediction was performed using the Backpropagation Neural Network method, resulting in the values shown in Tables 2 and 3.

Reviewing Tables 3 and 4, the results of the BPNN algorithm learning-prediction for each parameter can be observed, including Layer, Epoch, Learning rate, MAPE, and MSE during the learning and validation processes. The optimized architecture model in the learning phase, with a layer configuration of 8-8-10-5, a learning rate of 0.3, and an epoch of 9999, achieved excellent accuracy with an MSE value of 0.000716 and MAPE value of 5.43747. These parameters could also predict the validation data from 2016 to 2020 with reasonably good accuracy, resulting in a Validate MSE of 0.06555 and Validate MAPE of 45.63599. These results are quite good but slightly deviate from the ideal MAPE value as they are above 15%. This deviation was due to significant changes in the training-learning database pattern (2003-2015) compared to the validation period (2016-2020). According to Nayak (2023), this phenomenon is intimately tied to the more unpredictable climate circumstances induced by climate change and global warming. It is crucial to note that the accuracy of most composite models tends to decline as the projection period lengthens. As a result, the learning process satisfies the requirements for usage in the prediction process. However, the prediction phase requires additional modification, as it is the most crucial

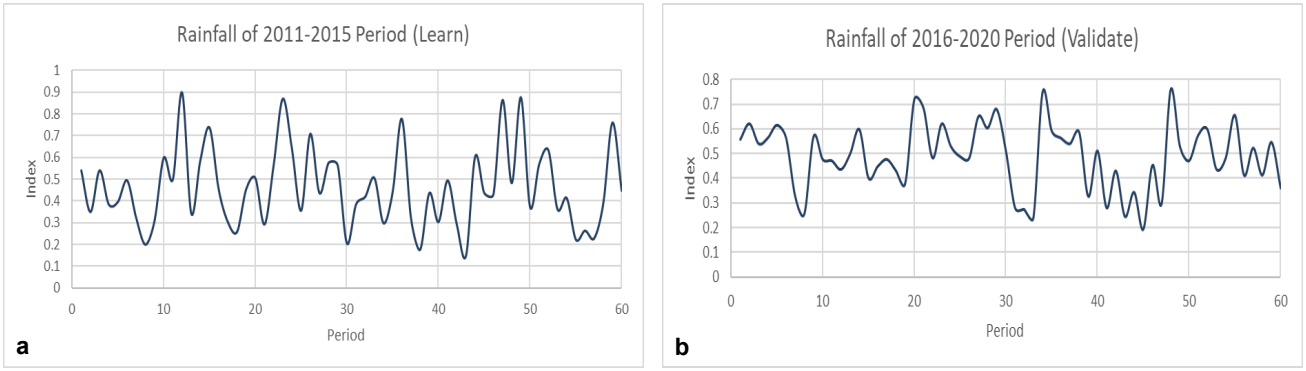

Fig. 2. (*a) Actual Rainfall Graph from 2011 to 2015 (Learn) (b) Rainfall graph for the period 2016-2020 (Validate)*

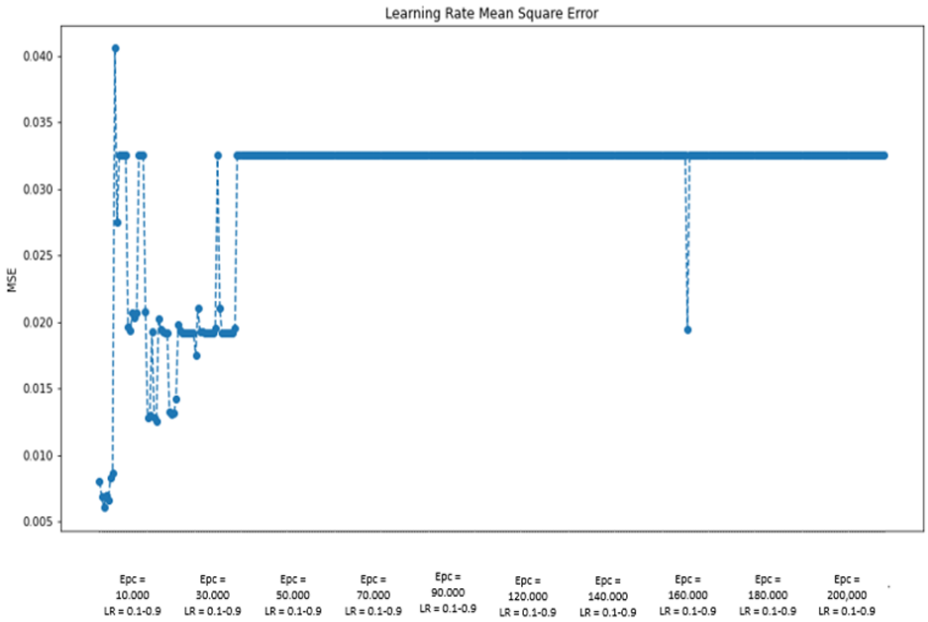

Fig. 3. *MSE graph depicting the link between epoch value and learning rate*

stage in forecasting rainfall patterns that may occur in Kapuas Hulu, West Kalimantan.

Specifically, in the BPNN information, the prediction process resulted in optimizing the architecture model with a configuration of 8-6-9-6-5, learning rate of 0.3, and epoch of 9999, achieving fairly good accuracy with an MSE value of 0.012157 and MAPE value of 24.02655. These figures are fairly good compared to the learning architecture model's correctness. However, they were not absolute for the validation data situation. Validated MSE and MAPE accuracy values for the Prediction Architecture Model were 0.03365 and 32.0862, respectively. When compared, the prediction architecture model (8-6-9-6-5) was much more predictable than the learning model (8-8-10-5). Fig. 4 depicts a comparison graph between the best architecture in the learning phase and the best architecture in the prediction process versus the actual/target values.

Spotlight on Fig. 4, the blue line represents the target data, the green line represents the learn model, and the yellow line represents the predict model. In general, both models have shown the pattern of rainfall prediction and learning that tends to follow the target data or validate data that occurred in Kapuas Hulu. However, there are shifting or peak shifts in certain time phases, such as August 2018-May 2019 and August 2016-

Table 3. *Best parameter of Learning rainfall with Backpropagation Neural Network (BPNN)*

Result of Variable	Value		
	Hidden Layer	**Neuron Hidden Layer**	**Architectures**
Layer	3	18	8-8-10-5
Epoch and Learning Rate	9999 and 0.3		
MAPE (%)	5.43747286185864		
MSE (%)	0.000716307355991353		
Validate MAPE (%)	45.6359956121716		
Validate MSE (%)	0.0655589932455263		

Table 4. Best *Parameter of Prediction rainfall with Backpropagation* Neural Network (BPNN)

Result of Variable	Value		
	Hidden Layer	**Neuron Hidden Layer**	**Architectures**
Layer	3	21	8-6-9-6-5
Epoch and Learning Rate	9999 and 0.3		
MAPE (%)	24.0265514508133		
MSE (%)	0.0121571836440613		
Validate MAPE (%)	32.086221264082		
Validate MSE (%)	0.0336559213805777		

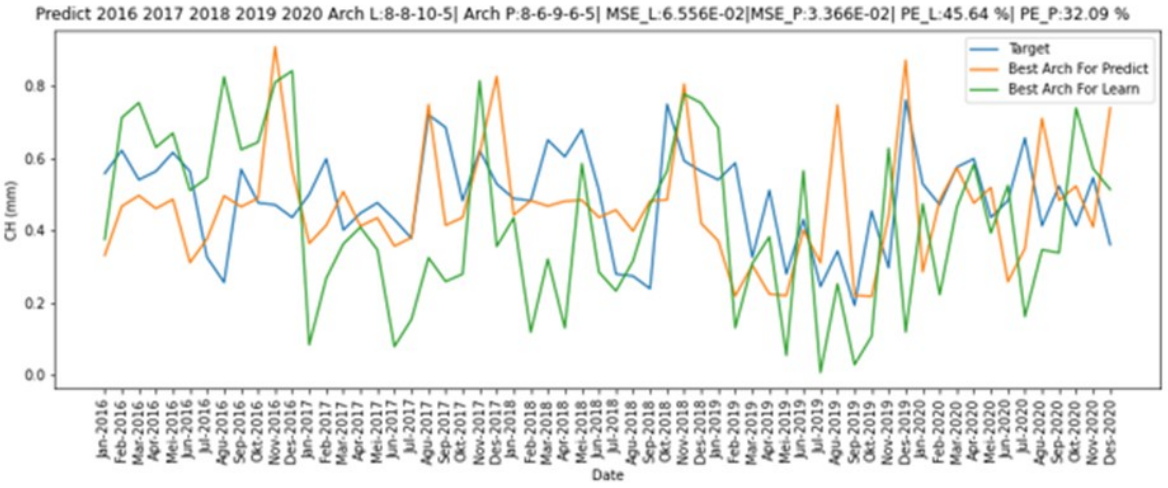

Fig. 4. *Graph of rainfall pattern all process predictions 2016-2020 (Data target = blue line), (green line = 8-8-10-5/Learn model), and (yellow line = 8-6-9-6-5/Predict Model)*

January 2017. Significant changes in the Training and Learning data with a propensity for the same or non-complex repeating patterns, as shown in Fig. 2(a) Training Data and 2(b) Validation Data, significantly impacted this. This has an impact on the results of the model in Fig. 4. The BPNN algorithm only remembers regular pattern shapes learned from the Training and Learning data. However, the results of these data changes are still capable enough to predict future climate pattern conditions, although not with 100% accuracy. This aligns with the report by Zhang *et al.*. (2023) that chaotic weather conditions cause weather sequences and patterns to always show firm peaks and fluctuations. These characteristics greatly affect the prediction accuracy of weather variables such as wind speed, solar intensity, and rainfall. Therefore, changes and differences in peaks/intensity are to be expected due to increasingly complex weather conditions resulting from various issues, including global warming and climate change.

The largest deviation occured from August 2016 to July 2017. The significant deviations in the learning and prediction models might be due to the learning process of the data from 2011 to 2015, as shown in Fig. 2(a). At the beginning of the graph pattern, there were no peaks or increases in rainfall data. Therefore, significant deviations were observed during the validation process, which only compares the data (without any learning process). However, these deviations are still tolerable. Hence, it can be inferred that an unusual natural phenomenon disrupts the rainfall pattern before and after that period.

Ensemble models' accuracy is based on the premise that the connections between multiple variables, such as temperature, rainfall, and atmospheric pressure, stay steady throughout time. However, if climate change accelerates, these linkages might alter in unforeseen ways, decreasing accuracy in ensemble models. As a result, when evaluating ensemble model findings and making judgments based on their forecasts, these circumstances must be taken into account. To increase the accuracy of long-term forecasts, other modeling techniques that explicitly account for the changing interactions between different variables in a changing climate may be required. Thus, with its high intensity, it is crucial to have a representative depiction of the rainfall patterns in Tanjug Beruang, West Kalimantan, to predict future rainfall patterns and implement various forms of mitigation. Table 5 displays the expected rainfall values for 2016-2020 using the 8- 6-9-6-5 Architectural model.

Table 5 shows the predicted rainfall results using the best architecture model, namely 8- 6-9-6-5, which has been denormalized to be equivalent to the monthly rainfall amounts from January 2016 to December 2020. The table depicts that the majority of maximum rainfall, which has the potential to cause floods and landslides, occurs in the Kapuas Hulu district of West Kalimantan

Table 5. Rainfall Prediction denormalization data for 2016-2020 (Validate)

Month	Year				
	2016 (mm)	**2017 (mm)**	**2018 (mm)**	**2019 (mm)**	**2020 (mm)**
Jan	430.1272054	379.6897826	369.598472	414.9950221	404.9037114
Feb	485,6150662	465.4420101	364.5575992	455.3506994	354.4662886
Mar	414.9950221	293.9375551	510.8385602	228.3583837	445.2593888
Apr	435.1776434	334.2932325	470.4828828	389.771528	465.4420101
May	480.5741935	359.5071613	536.052489	188.0122716	324.2019219
June	435.1776434	319.1610492	389.771528	319.1610492	364.5575992
July	228.3583837	273.7549338	188.0122716	157.7479049	515.8794329
August	167.8296503	571.3672936	182.9618336	243.4905671	304.0288658
Sept	440.2185161	541.1029269	152.6974669	112.3513548	399.8628387
Oct	359.5071613	364.5575992	596.5812224	339.3341052	304.0288658
Nov	354.4662886	485.6150662	460.3915721	203.1444549	420.0358948
Dec	324.2019219	404.9037114	435.1776434	606.6725331	258.6227505

from October to February. This is because, based on the standard set by Sohn *et al.*. (2020), floods typically occur when the rainfall intensity exceeds 450 mm/ month. Therefore, massive mitigation policies are necessary from October to March to prevent floods and landslides, ensure the safety of daily activities, and strengthen security in the border areas of the Republic of Indonesia.

Conclusion

The long-term Backpropagation Neural Network (BPNN) approach was used to predict rainfall in Kapuas Hulu, West Kalimantan Province. Based on the approach outcomes, the BPNN technique separated the Learning Phase into Training Data from January 2003 to December 2010, Learning Data from January 2011 to December 2015, and Validation/Prediction Data from January 2016 to December 2020. 8-6-9-6-5 was the best predictive/validation architectural model, with a learning rate 0.3 and an epoch of 9,999. The prediction accuracy was outstanding, with a Validate MSE of 0.0336559213805777 and a Validate MAPE of 32.086221264082.The highest rainfall was observed in December 2019, amounting to 606.6725331 mm. Therefore, the BPNN method can be considered one of the best alternatives for predicting rainfall in Kapuas Hulu, West Kalimantan Province, Indonesia, and can be used to mitigate future disasters such as flash floods and landslides. It is highly recommended that other relevant prediction methods/models/algorithms be used to enhance and validate the model's confidence.

Conflict of interest

The authors declare that they have no conflict of interest.

REFERENCES

1. Afolabi, H. A., & Aburas, A. (2021). Proposed back propagation deep neural network for intrusion detection in internet of things fog computing. *International Journal of Emerging Trends in Engineering Research*, 9(4), 464-469. https://doi.org/10.30534/ijeter/2021/23942021.
2. Al Mamun, A., Sohel, M., Mohammad, N., Sunny, M. S. H., Dipta, D. R., & Hossain, E. (2020). A comprehensive review of the load forecasting techniques using single and hybrid predictive models. *IEEE Access*, 8, 134911-134939. DOI:10.1109/ACCESS.2020.3010702.
3. Bapiyev, I. M., Aitchanov, B. H., Tereikovskyi, I. A., Tereikovska, L. A., & Korchenko, A. A. (2017). Deep neural networks in cyber attack detection systems. *International Journal of Civil Engineering and Technology (IJCIET)*, 8 (11), 1086-1092.
4. Chauhan, D., & Thakur, J. (2014). Data mining techniques for weather prediction: A review. *International Journal on Recent and Innovation Trends in Computing and Communication*, 2(8), 2184-2189. DOI: https://doi.org/10.17762/ijritcc.v2i8.3679.
5. Chen, G., Fu, K., Liang, Z., Sema, T., Li, C., Tontiwachwuthikul, P., & Idem, R. (2014). The genetic algorithm based back propagation neural network for MMP prediction in CO2- EOR process. *Fuel*, 126, 202-212. DOI : 10.1016/j.fuel.2014.02.034.
6. Fei, J., Zhao, N., Shi, Y., Feng, Y., & Wang, Z. (2016). Compressor performance prediction using a novel feedforward neural network based on Gaussian kernel function. *Advances in Mechanical Engineering*, 8(1). https://doi.org/10.1177/1687814016628396.
7. Guha, S., Jana, R. K., & Sanyal, M. K. (2022). Artificial neural network approaches for disaster management: A literature review (2010–2021). *International Journal of Disaster Risk Reduction*, 103276. DOI:10.1016/j.ijdrr.2022.103276.
8. Hanak, E., & Lund, J. R. (2012). Adapting California's water management to climate change.*Climate Change*, 111, 17-44. DOI:10.1007/s10584-011-0241-3

9. Karsoliya, S. (2012). Approximating number of hidden layer neurons in multiple hidden layer BPNN architecture. *International Journal of Engineering Trends and Technology*, 3(6), 714-717.
10. Kim, T., Ko, W., & Kim, J. (2019). Analysis and impact evaluation of missing data imputation in day-ahead PV generation forecasting. *Applied Sciences*, 9(1), 204. https://doi.org/10.3390/app9010204.
11. Kukreja, H., Bharath, N., Siddesh, C. S., & Kuldeep, S. (2016). An introduction to artificial neural network. *International Journal of Advance Research and Innovative Ideas in Education*, 1, 27-30.
12. Nayak, S. (2023). Exploring the Future Rainfall Characteristics over India from Large Ensemble Global Warming Experiments. *Climate*, 11(5), 94. https://doi.org/10.3390/cli11050094.
13. Oppenheimer, M., & Anttila-Hughes, J. K. (2016). The science of climate change. *The Future of Children*, 11-30. DOI : https://doi.org/10.1353/foc.2016.0001.
14. Pratama, M. B., Multazima, R., & Azkiarizqi, I. N. (2021). Hydro-Meteorological Aspects of the 2021 South Kalimantan Flood: Topography, Tides, and Precipitation. *International Journal of Remote Sensing and Earth Sciences* (IJReSES), 18(1), 73-90. DOI:10.31223/X5V89B
15. Putra, I. D. G. A., Nimiya, H., Sopaheluwakan, A., Kubota, T., Lee, H. S., Pradana, R. P., ... & Riama, N. F. (2022). Development of climate zones for passive cooling techniques in the hot and humid climate of Indonesia. *Building and Environment*, 226. DOI:10.1016/j.buildenv.2022.109698.
16. Qu, Z., Mao, W., Zhang, K., Zhang, W., & Li, Z. (2019). Multi-step wind speed forecasting based on a hybrid decomposition technique and an improved backpropagation neural network. *Renewable Energy*, 133, 919-929. DOI: 10.1016/j.renene.2018.10.043.
17. Rumelhart, D. E., Hinton, G. E., & Williams, R. J. (1986). Learning representations by back- propagating errors. *Nature*, 323(6088), 533-536. https://doi.org/10.1038/323533a0.
18. Salman, R. S. (2016). Impact Of El Nino Phenomenon On Paddy Field At Seram Island (Case Study: El Nino 2015-2016). *International Conference on Climate Change* (pp. 248- 254). https://doi.org/10.15608/iccc.y2016.570.
19. Shi, X., Chen, Z., Wang, H., Yeung, D. Y., Wong, W. K., & Woo, W. C. (2015). Convolutional LSTM network: A machine learning approach for precipitation nowcasting. Advances in neural information processing systems, 28. *NIPS*. https://doi.org/10/48550/arXiv.1506.04214.
20. Shihab, K. (2006). A backpropagation neural network for computer network security. *Journal of Computer Science*, 2(9), 710-715. DOI:10.3844/jcssp.2006.710.715.
21. Shirzadi, N., Nizami, A., Khazen, M., & Nik-Bakht, M. (2021). Medium-term regional electricity load forecasting through machine learning and deep learning. *Designs*, 5 (2), 27. https://doi.org/10.3390/designs5020027.
22. Sohn, W., Kim, J. H., Li, M. H., Brown, R. D., & Jaber, F. H. (2020). How does increasing impervious surfaces affect urban flooding in response to climate variability?. Ecological Indicators, 118, 106774. DOI:10.1016/j.ecolind.2020.106774.
23. Tarigan, J., Diedan, R., & Suryana, Y. (2017). Plate recognition using backpropagation neural network and genetic algorithm. *Procedia Computer Science*, 116, 365-372. https://doi.org/10.1016/j.procs.2017.10.068.
24. Todini, E. (2007). Hydrological catchment modelling: past, present and future. *Hydrology and Earth System Sciences*, 11(1), 468-482. https://doi.org/10.5194/hess-11-468-2007
25. VanDeventer, W., Jamei, E., Thirunavukkarasu, G. S., Seyedmahmoudian, M., Soon, T. K., Horan, B., ... & Stojcevski, A. (2019). Short-term PV power forecasting using hybrid GASVM technique. *Renewable Energy*, 140, 367-379. DOI: 10.1016/j.renene.2019.02.087.
26. Werbos, P. (1974). Beyond regression: New tools for prediction and analysis in the behavioral sciences. PhD thesis, Committee on Applied Mathematics, Harvard University, Cambridge, MA.
27. Wica, M., Witkowsk, M., Szumiec, A., & Ziebura, T. (2019). Weather forecasting system with the use of neural network and backpropagation algorithm. In Proceedings of the International Conference on Data Engineering and Communication Technology; Springer: Singapore (Vol. 2468, pp. 37-41).
28. Zhang, E., Hou, L., Shen, C., Shi, Y., & Zhang, Y. (2015). Sound quality prediction of (BPNN) based on particle swarm vehicle interior noise and mathematical modeling using a back propagation neural network optimization (PSO). *Measurement Science and Technology*, 27(1), 015801. DOI 10.1088/0957-0233/27/1/015801.
29. Zhang, J., Zhang, R., Zhao, Y., Qiu, J., Bu, S., Zhu, Y., & Li, G. (2023). Deterministic and Probabilistic Prediction of Wind Power Based on a Hybrid Intelligent Model. *Energies*, 16(10), 4237. https://doi.org/10.3390/en16104237.
30. Zhong, J., Liu, L., Sun, Q., & Wang, X. (2018). Prediction of photovoltaic power generation based on general regression and back propagation neural network. *Energy Procedia*, 152, 1224-1229. DOI:10.1016/j.egypro.2018.09.173.